The N2-dominated scenario of leptogenesis

PROCEEDINGS OF SCIENCE

The N_2-dominated scenario of leptogenesis

Michele Re Fiorentin*
Southampton U.

E-mail: m.re-fiorentin@soton.ac.uk

We briefly review the main aspects of leptogenesis, pointing out the main reasons that draw attention to the so-called N_2-dominated scenario. We consider the conditions that arise when the final asymmetry is required to be fully independent of the initial conditions. We show that in this scenario, called strong thermal leptogenesis, when barring special cancellations in the see-saw formula and in the flavoured decay parameters, a lightest neutrino mass $m_1 \gtrsim 10$ meV for normal ordering and $m_1 \gtrsim 3$ meV for inverted ordering are favoured. We shortly comment on the inclusion of corrective effects such as flavour coupling. We then focus on the $SO(10)$-inspired leptogenesis models that naturally realise N_2-dominated leptogenesis. We show that in this scenario, and even more in combination with the strong thermal leptogenesis conditions, important predictions on the neutrino parameters are obtained. We finally point out that these predictions will be in the reach of forthcoming experiments, thus enabling us to test $SO(10)$-inspired and strong thermal $SO(10)$-inspired leptogenesis.

Proceedings of the Corfu Summer Institute 2014
3-21 September 2014
Corfu, Greece

*Speaker.

1. Introduction

Leptogenesis is a particularly attractive way for producing the baryon asymmetry of the Universe, since it can be realised within the seesaw mechanism, in turn able to explain the observed neutrino masses and mixing.

We focus here on the standard type-I seesaw, with the inclusion of heavy right-handed (RH) Majorana neutrinos, N_{Ri}, that couple to the lepton doublets via Yukawa interactions:

$$\mathscr{L} = \mathscr{L}_{\rm SM} - Y_{D\alpha i}\ell_{L\alpha}N_{Ri}\tilde{\Phi} - \frac{1}{2}\overline{N_{Ri}^c}D_{Mi}N_{Ri} + \text{h.c.}, \tag{1.1}$$

where Y_D are the RH neutrinos Yukawa couplings and D_M is the diagonal Majorana mass matrix. When the RH neutrinos mass scale is much higher than the electroweak scale (the so called seesaw limit), the neutrino mass spectrum splits into two sets. The first one is made of light, Majorana, active neutrinos ν_i whose mass matrix is given by

$$m_\nu = -m_D D_M^{-1} m_D^T, \tag{1.2}$$

where $m_D \equiv vY_D$ is the Dirac neutrino mass matrix, proportional to the Higgs vacuum expectation value v. The eigenvalues of m_ν can be obtained as $D_m = -U^\dagger m_\nu U^*$ by means of the PMNS matrix U. Due to the interplay between the electroweak scale $v \sim 200\,\text{GeV}$ and the heavy Majorana neutrinos scale $M \gg v$, the active neutrinos masses $m_\nu \propto v^2/M$ turn out to be suitably small, without the need for artificially tuned Yukawa couplings.
The second set is composed of heavy Majorana neutrinos N_i, whose mass matrix basically coincides with D_M, up to negligible corrections.

This elegant way of generating small neutrino masses has however some drawbacks. The addition of heavy RH neutrinos introduces new free parameters to the model. For instance, if we assume, as we will always do in what follows, the presence of 3 RH neutrinos, the seesaw model depends on 18 free parameters that split into the 9 so-called *low-energy neutrino parameters,* probed in experiments, and a further 9 describing the high-energy scale of the heavy neutrinos. The seesaw mechanism on its own does not provide any explanation nor prediction on their values. In this regard, we can then either seek further theoretical input, or turn to an apparently unrelated phenomenology such as the baryon asymmetry of the Universe. This can be done by means of leptogenesis.

2. Leptogenesis

Leptogenesis [1] can be realised within a standard type-I seesaw model with the inclusion of at least 2 RH neutrinos. As already mentioned, in this work we shall consider 3 RH neutrinos. Their Majorana nature automatically ensures lepton-number violation. The presence in the seesaw lagrangian of Yukawa couplings to the left-handed lepton doublets allows the heavy neutrinos, through their RH component, to decay into leptons and antileptons. Due to complex Yukawa couplings and the interference between tree-level and one-loop diagrams, the heavy neutrinos decays are *CP*-violating.

CP-violation is estimated by the *CP*-asymmetry factors

$$\varepsilon_{i\alpha} \equiv -\frac{\Gamma_{i\alpha} - \bar{\Gamma}_{i\alpha}}{\sum_\beta \left(\Gamma_{i\beta} + \bar{\Gamma}_{i\beta}\right)}, \tag{2.1}$$

where $\Gamma_{i\alpha}$ ($\bar{\Gamma}_{i\alpha}$) are the zero-temperature decay rates of the heavy neutrino N_i into leptons (antileptons) of flavour α. Decays are also regulated by the so-called flavoured decay factors

$$K_{i\alpha} \equiv \frac{\Gamma_{i\alpha}}{H(T = M_i)}, \tag{2.2}$$

where $H(T = M_i)$ is the value of the Hubble parameter when N_i becomes non-relativistic. The decay factors $K_{i\alpha}$ do not only measure whether decays are in equilibrium at that epoch, but also give an estimate of the efficiency of the inverse decays, responsible for the production of N_i. Inverse decays are also the main source of washout of the generated asymmetry, therefore $K_{i\alpha}$ are a measure of the washout strength too.

When occurring out of equilibrium, heavy neutrino decays can produce a net lepton asymmetry. If this takes place at temperatures $T \gtrsim 100$ GeV, electroweak sphaleron processes are able to partly convert the lepton asymmetry into the baryon sector. Since both the baryon and lepton numbers are violated, but their difference $B - L$ is conserved by the sphaleron processes, we can quantify the asymmetry produced by leptogenesis as N_{B-L}, which can then be related to the baryon-to-photon ratio η_B as

$$\eta_B \simeq 0.96 \times 10^{-2} N_{B-L}. \tag{2.3}$$

Current CMB anisotropies measurements [2] precisely estimate the baryon-to-photon ratio as

$$\eta_B^{\rm CMB} = (6.1 \pm 0.1) \times 10^{-10}. \tag{2.4}$$

2.1 The N_2-dominated scenario

We focus, now, on a particular hierarchical heavy neutrino spectrum with

$$M_1 \lesssim 10^9\,\text{GeV} \lesssim M_2 \lesssim 10^{12}\,\text{GeV} \lesssim M_3. \tag{2.5}$$

Since N_3 is the heaviest neutrino, it is either non-thermalised or its *CP*-asymmetry is too low, therefore its contribution to the asymmetry is negligible. Similarly for N_1, which is too light. For this reason, the final asymmetry is mainly produced by the next-to-lightest heavy neutrino and this scenario takes the name N_2-*dominated* [3]. If flavour interactions are completely neglected, heavy neutrinos decay into a coherent superposition of flavour eigenstates, producing an (unflavoured) asymmetry

$$N_{B-L}^{\rm lep,f} \simeq \varepsilon_2\, \kappa(K_2) e^{-\frac{3\pi}{8} K_1}. \tag{2.6}$$

Here $\kappa(K_2)$ is the efficiency factor at the production [4]. The final value of the asymmetry is exponentially suppressed by N_1's washout. Only when $K_1 \ll 1$ the model can produce the observed asymmetry. A numerical analysis shows that this is realised in only $\sim 0.2\%$ of the parameter space [5, 6].

This picture improves by taking account of flavour interactions. Considering that τ-interactions are efficient for $T \lesssim 10^{12}$ GeV, and muonic ones for $T \lesssim 10^9$ GeV, and given the heavy neutrino

spectrum as in eq. (2.5), N_2 decays in a two fully-flavoured regime, while the washout due to N_1 takes place in a three fully-flavoured regime. Around the transition temperatures, the behaviour cannot be described by Boltzmann equations and a full density matrix formalism must be adopted [7]. Avoiding these regions, N_1's washout acts separately on each flavour $\alpha = e, \mu, \tau$, exponentially suppressing the asymmetry by the relative flavoured decay parameter $K_{1\alpha}$ [8]. We have

$$\begin{aligned} N_{B-L}^{\rm lep,f} \simeq & \left[\frac{K_{2e}}{K_{2\tau_2^\perp}}\varepsilon_{2\tau_2^\perp}\kappa(K_{2\tau_2^\perp}) + \left(\varepsilon_{2e} - \frac{K_{2e}}{K_{2\tau_2^\perp}}\varepsilon_{2\tau_2^\perp}\right)\kappa(K_{2\tau_2^\perp}/2)\right] e^{-\frac{3\pi}{8}K_{1e}} \\ & + \left[\frac{K_{2\mu}}{K_{2\tau_2^\perp}}\varepsilon_{2\tau_2^\perp}\kappa(K_{2\tau_2^\perp}) + \left(\varepsilon_{2\mu} - \frac{K_{2\mu}}{K_{2\tau_2^\perp}}\varepsilon_{2\tau_2^\perp}\right)\kappa(K_{2\tau_2^\perp}/2)\right] e^{-\frac{3\pi}{8}K_{1\mu}} \\ & + \varepsilon_{2\tau}\kappa(K_{2\tau})e^{-\frac{3\pi}{8}K_{1\tau}}, \end{aligned} \tag{2.7}$$

where $\varepsilon_{2\tau_2^\perp} \equiv \varepsilon_{2e} + \varepsilon_{2\mu}$ and similarly $K_{2\tau_2^\perp} \equiv K_{2e} + K_{2\mu}$. As can be noticed, it is sufficient that only one $K_{1\alpha}$ is smaller than 1 in order to have enough asymmetry produced. This is found to happen in $\sim 30\%$ of the parameter space, showing that thanks to flavour effects the N_2-dominated scenario can represent a viable model of leptogenesis.

The second term in each square bracket in eq. (2.7) is the so called *phantom term*. These are effects due to the different flavour compositions of the lepton $|\ell_2\rangle$ and anti-lepton $|\bar{\ell}_2\rangle$ states produced by the decay of N_2 and give a correction to the final asymmetry. For convenience, we have neglected this effect in the rest of this work.

3. Strong thermal leptogenesis

The final baryon asymmetry depends in general on the initial conditions. Moreover, the high reheating temperatures $T_{\rm RH} \gtrsim 10^{12}\,{\rm GeV}$ required by this scenario of thermal leptogenesis, see eq. (2.5), allow several mechanism (e.g. GUT- [9], gravitational- [10], Affleck-Dine- [11] baryogenesis) to produce a rather high asymmetry. This asymmetry is produced before the onset of leptogenesis, and is referred to as *initial pre-existing asymmetry*, $N_{B-L}^{\rm p,i}$. At lower temperatures, leptogenesis takes place and in general it modifies this asymmetry to a final value $N_{B-L}^{\rm p,f}$. We can require

$$N_{B-L}^{\rm p,f} \ll N_{B-L}^{\rm lep,f} \simeq N_{B-L}^{\rm CMB}\,, \tag{3.1}$$

namely that the final pre-existing asymmetry is negligible in comparison to the asymmetry produced by leptogenesis, $N_{B-L}^{\rm lep,f}$, which therefore genuinely constitutes the amount of asymmetry measured today. In this way, full independence of the initial conditions is ensured and leptogenesis is said to satisfy the *strong thermal* condition [13]. It has been shown [13] that strong thermal leptogenesis can be realised with hierarchical heavy neutrino spectra[1], but only in a two-stage process where the heavy neutrinos show a spectrum as in eqs. (2.5). This is one of the main reasons why the N_2-dominated scenario is important. The final value of the pre-existing asymmetry is given

[1] As for degenerate heavy neutrino spectra, a computation with full density matrices is needed to clarify if strong thermal leptogenesis can actually be realised.

by [13, 14]

$$N_{B-L}^{\rm p,f} \simeq \Bigg\{ \left[(1-p_{\rm p\tau}) \left[p_{\rm p\tau_2^\perp} \frac{K_{2e}}{K_{2\tau_2^\perp}} e^{-\frac{3\pi}{8} K_{2\tau_2^\perp}} + \left(1-p_{\rm p\tau_2^\perp}\right) \left(1-\frac{K_{2e}}{K_{2\tau_2^\perp}}\right) \right] + \Delta p_{\rm pe} \right] e^{-\frac{3\pi}{8} K_{1e}}$$
$$+ \left[(1-p_{\rm p\tau}) \left[p_{\rm p\tau_2^\perp} \frac{K_{2\mu}}{K_{2\tau_2^\perp}} e^{-\frac{3\pi}{8} K_{2\tau_2^\perp}} + \left(1-p_{\rm p\tau_2^\perp}\right) \left(1-\frac{K_{2\mu}}{K_{2\tau_2^\perp}}\right) \right] + \Delta p_{\rm p\mu} \right] e^{-\frac{3\pi}{8} K_{1\mu}}$$
$$+ (p_{\rm p\tau} + \Delta p_{\rm p\tau}) e^{-\frac{3\pi}{8}(K_{2\tau}+K_{1\tau})} \Bigg\} N_{B-L}^{\rm p,i}, \tag{3.2}$$

where $p_{\rm p\tau}$ and $p_{\rm p\tau_2^\perp}$ are the fractions of the pre-existing asymmetry in the τ and $\tau_2^\perp$ components respectively. The terms $\Delta p_{\rm p\alpha}$, with $\sum_\alpha \Delta p_{\rm p\alpha} = 0$, describe the possible different flavour composition of the initial pre-existing asymmetry. In this scenario, N_2 decays in the two-flavoured regime and efficiently washes out the τ component of $N_{B-L}^{p,i}$ with a large $K_{2\tau}$. On the other hand, N_1 decays in the three-flavoured regime, separately erasing the e and μ components of $N_{B-L}^{p,i}$, while the asymmetry produced by N_2 survives in the τ flavour. This translates into a set of conditions on the relevant decay parameters

$$K_{1e}, K_{1\mu}, K_{2\tau} \gg 1, \quad K_{1\tau} \lesssim 1. \tag{3.3}$$

When these conditions are imposed on the requirement of successful leptogenesis (i.e. $\eta_B^{\rm lep} \simeq \eta_B^{\rm CMB}$) a precise analytical lower bound on the absolute mass scale m_1 appears [15]. Adopting the Casas-Ibarra parameterisation [16], we introduce a complex orthogonal matrix $\Omega = D_m^{-1/2} U^\dagger m_D D_M^{-1/2}$, that links the low-energy (neutrino masses and mixing) and the high-energy (heavy neutrinos) parameters. In this way, the expression for the decay parameters becomes

$$K_{i\alpha} = \left| \sum_j \sqrt{\frac{m_j}{m_*}} U_{\alpha j} \Omega_{ji} \right|^2, \tag{3.4}$$

where $m_* \simeq 1.1 \times 10^{-3}\,\text{eV}$ is the equilibrium neutrino mass. Considering low values of m_1, that is $m_1 \lesssim m_{\rm sol}$, we can simplify the expression for $K_{1\alpha}$

$$K_{1\alpha} \simeq \left| \sqrt{\frac{m_1}{m_*}} U_{\alpha 1} \Omega_{11} + \sqrt{\frac{m_{\rm sol}}{m_*}} U_{\alpha 2} \Omega_{21} + \sqrt{\frac{m_{\rm atm}}{m_*}} U_{\alpha 3} \Omega_{31} \right|^2. \tag{3.5}$$

Specifying $\alpha = \tau$, we obtain

$$\sqrt{\frac{m_{\rm atm}}{m_*}} U_{\tau 3} \Omega_{31} = -\sqrt{\frac{m_1}{m_*}} U_{\tau 1} \Omega_{11} - \sqrt{\frac{m_{\rm sol}}{m_*}} U_{\tau 2} \Omega_{21} + \sqrt{K_{1\tau}} e^{i\varphi_\tau}, \tag{3.6}$$

and substitute it in the expression for $K_{1\gamma}$, with $\gamma = e, \mu$

$$K_{1\gamma} = \left| \Omega_{11} \sqrt{\frac{m_1}{m_*}} \left(U_{\gamma 1} - \frac{U_{\tau 1}}{U_{\tau 3}} U_{\gamma 3} \right) + \sqrt{K_{1\gamma}^0} e^{i\varphi_0} \right|^2. \tag{3.7}$$

Here $K_{1\gamma}^0 \equiv K_{1\gamma}(m_1 = 0)$, so that

$$\sqrt{K_{1\gamma}^0} e^{i\varphi_0} \equiv \Omega_{21} \sqrt{\frac{m_{\rm sol}}{m_*}} \left(U_{\gamma 2} - \frac{U_{\tau 2}}{U_{\tau 3}} \right) + \frac{U_{\gamma 3}}{U_{\tau 3}} \sqrt{K_{1\tau}} e^{i\varphi_\tau}. \tag{3.8}$$

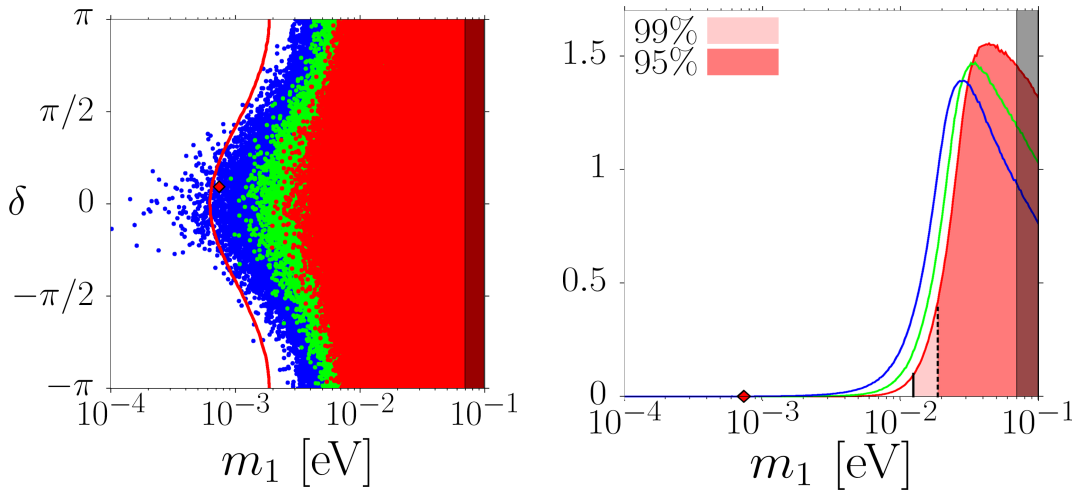

(a) (b)

Figure 1: (a) Scatter plot of successful strong leptogenesis models. Initial pre-existing asymmetries are $N^{\mathrm{p,i}}_{B-L} = 0.1, 0.01, 0.001$ respectively in red, green and blue. The solid line is the 95% confidence level analytical lower bound. (b) Distribution of probability of m_1 from the scatter plot, colour code as in (a). The red diamond marks the analytical lower bound. These models have $M_\Omega = 2$ [15].

We can take the size of the entries of the orthogonal matrix to be in general $\left|\Omega_{ij}\right|^2 \leq M_\Omega$. Usually $M_\Omega = \mathcal{O}(1)$, so that the seesaw mechanism truly relies on the interplay between the electroweak and the Majorana scales, rather than on fine-tuned cancellations. This way, the maximum values of $K_{1\gamma}$ are obtained for

$$K^{\max}_{1\gamma} = \left(M_\Omega \sqrt{\frac{m_1}{m_*}} \left| U_{\gamma 1} - \frac{U_{\tau 1}}{U_{\tau 3}} U_{\gamma 3} \right| + \sqrt{K^{0,\max}_{1\gamma}} \right)^2 , \tag{3.9}$$

with

$$\sqrt{K^{0,\max}_{1\gamma}} \equiv M_\Omega \sqrt{\frac{m_{\mathrm{sol}}}{m_*}} \left| U_{\gamma 2} - \frac{U_{\tau 2}}{U_{\tau 3}} \right| + \left| \frac{U_{\gamma 3}}{U_{\tau 3}} \right| \sqrt{K^{\max}_{1\tau}} . \tag{3.10}$$

The strong thermal leptogenesis conditions in eq. (3.3) can be specified by using the general relation in eq. (3.1). For each flavour we must have $N^{\mathrm{p,f}}_{\Delta\alpha} < \zeta N^{\mathrm{lep,f}}_{\Delta\alpha}$, with $\zeta \ll 1$, where $N^{\mathrm{p,i}}_{\Delta\alpha}$ is the fraction of pre-existing asymmetry in the flavour α. Since the washout takes place exponentially, we can define

$$K_{\mathrm{st}}\left(N^{\mathrm{p,i}}_{\Delta\alpha}\right) \equiv \frac{3}{8\pi} \left[\ln\left(\frac{100\zeta}{N^{\mathrm{CMB}}_{B-L}} \right) + \ln\left|N^{\mathrm{p,i}}_{\Delta\alpha}\right| \right] \simeq 18 + 0.85 \left(\ln\zeta + \ln\left|N^{\mathrm{p,i}}_{\Delta\alpha}\right| \right) , \tag{3.11}$$

and so we must require for each flavour $\gamma = e, \mu$

$$K_{1\gamma} \gtrsim K_{\mathrm{st}}(N^{\mathrm{p,i}}_{\Delta\gamma}) . \tag{3.12}$$

This in turn implies $K_{1\gamma}^{\max} > K_{\rm st}(N_{\Delta\gamma}^{\rm p,i})$, namely

$$\left(M_\Omega\sqrt{\frac{m_1}{m_*}}\left|U_{\gamma 1}-\frac{U_{\tau 1}}{U_{\tau 3}}U_{\gamma 3}\right|+\sqrt{K_{1\gamma}^{0,\max}}\right)^2 > K_{\rm st}(N_{\Delta\gamma}^{\rm p,i}). \tag{3.13}$$

Solving with respect to m_1, we finally obtain

$$m_1 > m_1^{\rm lb} \equiv \frac{m_*}{M_\Omega}\max_\gamma\left[\left(\frac{\sqrt{K_{\rm st}(N_{\Delta\gamma}^{\rm p,i})}-\sqrt{K_{1\gamma}^{0,\max}}}{\left|U_{\gamma 1}-\frac{U_{\tau 1}}{U_{\tau 3}}U_{\gamma 3}\right|}\right)^2\right], \tag{3.14}$$

when

$$K_{1\gamma}^{0,\max} < K_{\rm st}(N_{\Delta\gamma}^{\rm p,i}). \tag{3.15}$$

For normal ordering, the maximum value is obtained for $\gamma = e$. Moreover, by imposing the other strong thermal condition, i.e. $K_{1\tau} \lesssim 1$, the condition in eq. (3.15) can be satisfied and a lower bound on m_1 can actually be found. Considering $M_\Omega = 2$, $N_{B-L}^{\rm p,i} = 0.1$, taking the experimental values of the mixing angles and $\delta = 0$ we have $m_1^{\rm lb} \simeq 0.7\,{\rm meV}$. In fig. 1(a) we show the scatter plot of points corresponding to successful strong thermal leptogenesis models able to efficiently washout a pre-existing asymmetry $N_{B-L}^{\rm p,i} = 0.001, 0.01, 0.1$ respectively in blue, green and red points. These models all have $M_\Omega = 2$. The solid red band is the analytical lower bound as in eq. (3.14), at 95% confidence level on the mixing parameters.

This analytical lower bound holds similarly for inverted ordering, but in this case it is generally much looser, due to the replacement $m_{\rm sol} \to m_{\rm atm}$. More precisely, an analytical lower bound on m_1 holds for IO only when $M_\Omega \lesssim 0.9$ and is therefore much looser than for NO.

From a statistical analysis of the simulations, we have noticed that the actual analytical lower bound is hardly saturated. On the contrary, strong thermal leptogenesis models tend to prefer rather high values of the absolute neutrino mass scale. The distribution of probability of m_1 corresponding to a model with $M_\Omega = 2$ (as in the scatter plot in fig. 1(a)) is shown in fig. 1(b). In general, for natural values of M_Ω (i.e. $M_\Omega \leq 4$), around 99% of models have $m_1 \gtrsim 10\,{\rm meV}$ in NO, while for IO the statistical limit is looser and 99% of models show $m_1 \gtrsim 3\,{\rm meV}$.

This result is particularly interesting since it provides us with a precise prediction that makes leptogenesis, in its strong thermal version, testable at future experiments. It can face many evidences from cosmological observations, however, the sensitivity is not yet sufficient to reasonably discriminate from the hierarchical ($m_1 = 0$) limit. This scenario will improve in forthcoming experiments, if a precision $\delta(\sum m_{\nu_i}) \lesssim 10\,{\rm meV}$ is reached [17]. In this case, measurements of the sum of the neutrino masses will be able to either support or severely corner strong thermal leptogenesis. It must be noticed that it is particularly important that long-baseline neutrino oscillation experiments determine the ordering. As we have seen, NO and IO show rather different features and, in particular, the lower bound for IO is much looser.

It can be convenient to point out once again how the simple requirement of full independence of the initial conditions can lead us to interesting constraints on the absolute neutrino mass scale, thus putting strong thermal leptogenesis within the experimental reach.

3.1 Strong thermal leptogenesis and flavour coupling

In eqs. (2.7) and (3.2) the evolution of the asymmetries in each flavour is totally independent. This is actually an approximation, because in reality the different flavour asymmetries are linked to each other by means of the asymmetries stored in the quark sector and in the Higgs doublet [12]. This effect is called *flavour coupling* and, when taken into account, makes strong thermal leptogenesis more stringent.

We can distinguish two kinds of flavour coupling: the flavour coupling that modifies the asymmetry at the production, i.e. at N_2's decay, and the one that influences the washout by N_1. It turns out that when strong thermal leptogenesis is considered, the most important effect is due to the flavour coupling at N_1's washout, while the coupling at the production can be safely neglected. In this case the produced asymmetry is given by [18]

$$N_{B-L}^{\rm lep,f} \simeq \left(1 - C_{e\tau}^{(3)} - C_{\mu\tau}^{(3)}\right) \varepsilon_{2\tau}\kappa(K_{2\tau}) e^{-\frac{3\pi}{8}K_{1\tau}}, \tag{3.16}$$

where $C_{\alpha\beta}^{(3)}$ is the matrix that couples the different flavour asymmetries in the three fully-flavoured regime. We have, in the end, that the final produced asymmetry is reduced by around 40% with respect to the uncoupled one, as can be seen in fig. 2. Flavour coupling also strengthens the strong

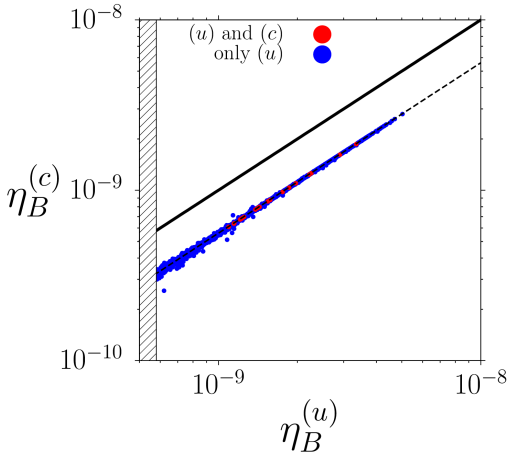

Figure 2: Plot of the baryon-to-photon ratio $\eta_B^{(c)}$ computed in flavour-coupled strong thermal leptogenesis versus $\eta_B^{(u)}$ computed from the same setup, but in the uncoupled regime. The initial pre-existing asymmetry required to wash out is $N_{B-L}^{\rm p,i} = 10^{-3}$. Blue dots indicate models in which strong thermal leptogenesis is successful only in the uncoupled (u) regime, while red points denote models in which strong thermal leptogenesis is realised both in the uncoupled and in the coupled regimes. The solid line represents $\eta_B^{(c)} = \eta_B^{(u)}$, while the dashed line $\eta_B^{(c)} = (1 - C_{e\tau}^{(3)} - C_{\mu\tau}^{(3)})\eta_B^{(u)}$. The part if the plot corresponding to $\eta_B^{(u)} \leq 5.8 \times 10^{-10}$ has been hatched away.

thermal conditions, requiring $K_{2\tau_2^\perp} \gg 1$ and $K_{1\tau} \ll 1$. This is due to the suppression of those asymmetry along e and μ that try to escape N_1's washout in the τ component.

As a result of flavour coupling, the analytical lower bound in eq. (3.14) is unchanged, however the statistical bounds are much stronger. The ratio between the mass bound realised in 99% of the

coupled models to that obtained in uncoupled models is always around a factor $2 \sim 3$ for different values of $N^{\rm p,i}_{B-L}$ [18].

4. $SO(10)$-inspired leptogenesis

As already mentioned, the attractive features of the seesaw mechanism rely on the addition of extra particles. These particles are somehow added by hand to the SM lagrangian and so is their high mass scale. A more elegant origin of the RH neutrinos and their mass scale can be found in Grand Unified Theories (GUT). In particular, it can be noticed that models based on $SO(10)$ as unification group [19], naturally include three RH neutrinos in the same irreducible representation together with quarks and leptons. RH neutrinos precisely fit in the 16-dimensional spinor representation of $SO(10)$ and their mass scale is linked to low-energy parameters, such as the Dirac neutrino mass matrix m_D and the PMNS mixing matrix U. With this in mind, it can be interesting to apply some conditions, that are directly inspired to $SO(10)$ GUT models, to leptogenesis. In particular:

- diagonalising the Dirac mass matrix as $m_D = V_L^\dagger D_{m_D} U_R$, the diagonal matrix is set to

$$D_{m_D} = \text{diag}\left(\alpha_1 m_u,\, \alpha_2 m_c,\, \alpha_3 m_t\right), \tag{4.1}$$

  where m_u, m_c, m_t are the up-quark masses at the leptogenesis scale,

- the proportionality constants are fixed to be $0.1 \lesssim \alpha_i \lesssim 10$,

- the unitary matrix V_L is set to be $\mathbb{1} \leq V_L \lesssim V_{\rm CKM}$, where $V_{\rm CKM}$ is the Cabibbo-Kobayashi-Maskawa quark mixing matrix.

Barring special crossing-level solutions, we have that the heavy neutrino spectrum is hierarchical and the scenario is N_2-dominated. By imposing these relations, several precise predictions on the heavy neutrino mass spectrum and the low-energy neutrino parameters can be obtained. These are strengthened if the strong thermal leptogenesis conditions in eq. (3.3) are taken into account at the same time. Considering strong thermal $SO(10)$-inspired leptogenesis, numerical simulations [14] have pointed out the following list of results.

i) The ordering of the active neutrino spectrum must be normal,

ii) the absolute neutrino mass scale is $m_1 \simeq 20\,\text{meV}$,

iii) the neutrinoless double-beta decay ($0\nu\beta\beta$) effective neutrino mass is found to be $m_{ee} \equiv |m_{\nu ee}| \simeq 0.8\, m_1 \simeq 15\,\text{meV}$,

iv)[2] a lower bound on the reactor mixing angle is found $\theta_{13} \gtrsim 2^\circ (0.5^\circ)$ for $N^{\rm p,i}_{B-L} = 10^{-1}(10^{-2})$,

v) an upper bound on the atmospheric mixing angle is found $\theta_{23} \lesssim 41^\circ (43^\circ)$ for $N^{\rm p,i}_{B-L} = 10^{-1}(10^{-2})$,

vi) the Dirac CP-violating phase must take values $\delta \in [-\pi/2, \pi/5]$ for $N^{\rm p,i}_{B-L} = 10^{-1}$, while for $N^{\rm p,i}_{B-L} = 10^{-2}$ we have $\delta \notin [0.4, 0.7]\pi$,

[2] This lower bound was found in [20], before the measurement by DayaBay [21].

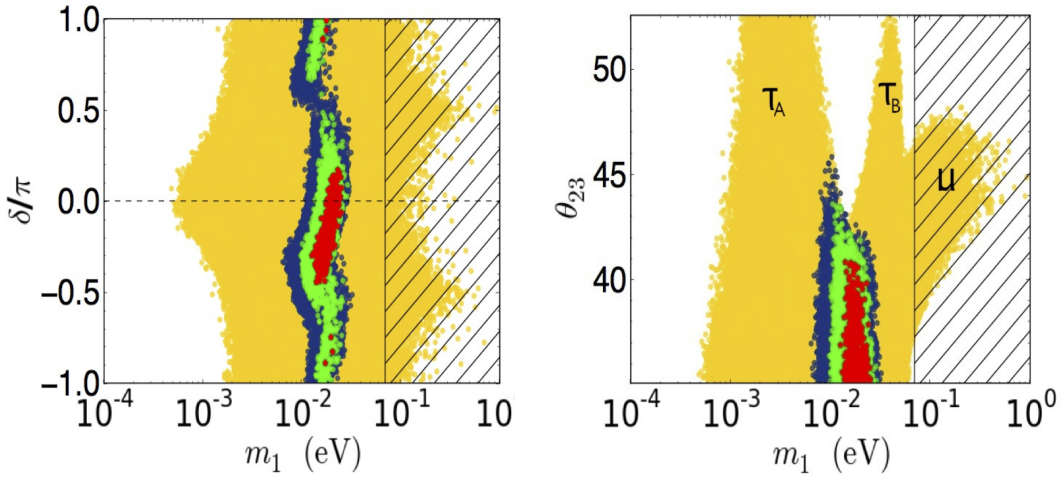

(a) (b)

Figure 3: Scatter plot of successful $SO(10)$-inspired, strong thermal leptogenesis models in the plane (m_1, δ), fig. (a), and (m_1, θ_{23}) in (b). Yellow, blue, green and red dots correspond to $N^{\mathrm{p,i}}_{B-L} = 0, 10^{-3}, 10^{-2}, 10^{-1}$. Notice the predicted values of m_1, δ and θ_{23} for $N^{\mathrm{p,i}}_{B-L} = 0.1$ [14].

vii) the Majorana phases tend to cluster around $(\sigma, \rho) \simeq (0.8+n, 1.25+n)\pi$ or $(\sigma, \rho) \simeq (0.7+n, 0.75+n)\pi$, with $n = 0, 1$.

In general, we can notice that prediction (ii) is consistent with the lower bound in eq. (3.14) from strong thermal leptogenesis.

Most importantly, $SO(10)$ is responsible for the upper bound on θ_{23}, that is then constrained to the value in (v) by strong thermal conditions. This prediction is particularly interesting, together with the value of δ given by (vi), and are shown in fig. 3. They both provide us with definite values that can be tested at the experiments. The value in (vi) is intriguingly in very good agreement with the current central value of the neutrino global fits [22, 23] and will be tested in long-baseline neutrino oscillation experiments (e.g. NOνA). On the other hand, the octant of θ_{23} is still very unstable.

A detailed study of $SO(10)$-inspired leptogenesis [24] analytically derived the bounds on the low-energy neutrino parameters coming from $SO(10)$ and strong thermal conditions, and confirmed all the results already obtained numerically [14].

We shall first consider plain $SO(10)$-inspired leptogenesis, analysing the impact of the strong thermal condition later.

It can be shown that for $V_L = \mathbb{1}$ and order unity values of α_i, the N_2 CP-asymmetries follow a hierarchical pattern as

$$\varepsilon_{2\tau} : \varepsilon_{2\mu} : \varepsilon_{2e} = \alpha_3^2 m_t^2 : \alpha_2^2 m_c^2 : \alpha_1^2 m_u^2 \, \frac{\alpha_3 m_t}{\alpha_2 m_c} \, \frac{\alpha_1^2 m_u^2}{\alpha_2^2 m_c^2}, \tag{4.2}$$

so that the final asymmetry is generally τ-dominated. This is certainly true for $V_L = \mathbb{1}$ and NO, while for $V_L \neq \mathbb{1}$, and especially in IO, this hierarchy is slightly modified and there can be solution with $|\varepsilon_{2\mu}| \sim |\varepsilon_{2\tau}|$. Avoiding this particular situation, a fully analytical expression for the final

asymmetry in the N_2-dominated scenario is obtained when $V_L = \mathbb{1}$

$$N_{B-L}^{\rm lep,f} \simeq \frac{3}{16\pi}\frac{\alpha_2^2 m_c^2}{v^2}\frac{|m_{ve e}|\left(\left|m_{\nu\tau\tau}^{-1}\right|^2+\left|m_{\nu\mu\tau}^{-1}\right|^2\right)^{-1}}{m_1 m_2 m_3}\frac{\left|m_{\nu\tau\tau}^{-1}\right|^2}{\left|m_{\nu\mu\tau}^{-1}\right|^2}\sin\alpha_L \\ \times\kappa\left(\frac{m_1 m_2 m_3}{m_*}\frac{\left|m_\nu^{-1}\right|^2}{\left|m_{ve e}\, m_{\nu\tau\tau}^{-1}\right|}\right)\exp\left\{-\frac{3\pi}{8}\frac{|m_{ve\tau}|^2}{m_*\,|m_{ve e}|}\right\}, \tag{4.3}$$

where

$$\alpha_L = \arg\left[m_{ve e}\right] - 2\arg\left[m_{\nu\mu\tau}^{-1}\right] - 2(\rho+\sigma) + \pi, \tag{4.4}$$

is the *effective leptogenesis phase*. This phase determines the sign of the final asymmetry. From eq. (4.3), it is possible to notice that the asymmetry is independent of α_1 and α_3 and that the neutrinos double-beta decay effective mass $m_{ee} \equiv |m_{ve e}|$ cannot be zero if a non-vanishing asymmetry is required. This equation is valid both in normal and inverted ordering, as long as the relevant parameters are specified accordingly. However, a modification is necessary to take into account IO solutions in which the μ asymmetry happens to be significant.

From eq. (4.3), it is possible to derive several bounds on the low-energy neutrino parameters, different in NO and in IO, which directly come from the $SO(10)$-inspired conditions.

As for normal ordering, the absolute neutrino mass scale m_1 must lie between two definite bounds

$$0.08\,\text{meV}\left(\frac{5}{\alpha_2}\right)^2 \lesssim m_1 \lesssim m_*\left[\frac{2.5^{1.2}\times 10^8}{192\pi}\frac{\alpha_2^2 m_c^2}{v^2}\right] \lesssim 52\,\text{meV}, \tag{4.5}$$

while there exists an upper bound on the atmospheric mixing angle

$$\theta_{23} \lesssim \arctan\left[\frac{m_{\rm atm} - m_{\rm sol}\, s_{12}^2}{m_{\rm sol}+m_1}\frac{s_{13}}{c_{12}\, s_{12}}\right] \lesssim 65^\circ. \tag{4.6}$$

It is also important to point out that a link between the sign of the asymmetry and the Dirac *CP* phase δ, which is forced to lie mainly in the fourth quadrant, can be derived. In general, the sign of the asymmetry influences the values of the phases, constraining also the Majorana phases ρ and σ.

When imposing the strong thermal leptogenesis conditions, the bounds on the low-energy parameters become even more stringent. In particular, requiring eq. (3.12) on K_{1e} we directly obtain a lower bound on the effective $0\nu\beta\beta$ decay mass. Indeed we have

$$m_{ee} \gtrsim 8\,\text{meV}\left(1 + 0.095\ln\left|\frac{N_{\Delta e}^{\rm p,i}}{1.5\times 10^{-4}}\right|\right), \tag{4.7}$$

which shows that, despite neutrino masses being NO, next generation $0\nu\beta\beta$ experiments should find a signal. This lower bound gives a lower bound on the absolute neutrino mass scale

$$m_1 \gtrsim 10\,\text{meV}\left(1 + 0.095\ln\left|\frac{N_{\Delta e}^{\rm p,i}}{1.5\times 10^{-4}}\right|\right), \tag{4.8}$$

that translates into a lower bound on the sum of the neutrino masses $\sum_i m_i \gtrsim 75\,\text{meV}$, which will be tested by future cosmological observations.

The absolute neutrino mass scale is also tightly connected to the atmospheric mixing angles, so that the minimum value of θ_{23} implies an upper bound on m_1. For $N^{\mathrm{p,i}}_{\Delta e} = 10^{-3}$ we have $\theta_{23} \lesssim 40^\circ$, thus giving $m_1 \lesssim 20\,\mathrm{meV}$, which is in good agreement with the numerical results (see blue points in fig. 3).

Imposing the strong thermal condition on $K_{1\mu}$ would imply $m_1 \gtrsim 30\,\mathrm{meV}$, for $N^{\mathrm{p,i}}_{\Delta\mu} = 10^{-3}$ and $\theta_{13} = 0^\circ$. Clearly this is incompatible with the previous upper bound, therefore, strong thermal leptogenesis necessarily requires a non-vanishing reactor mixing angle. For $\theta_{13} > 0^\circ$ the bounds obtained from K_{1e} and $K_{1\mu}$ are reconciled. We can conclude that strong thermal solutions predict nonzero reactor mixing angle [25], as now firmly established by experimental results and global analyses.

5. Conclusions

We have presented the results obtained in type-I seesaw, thermal leptogenesis when additional conditions are imposed. In the first part we have studied the impact of the strong thermal leptogenesis conditions on the low-energy neutrino parameters, also discussing some corrective effects such as flavour-coupling. In the second part we have analysed the leptogenesis scenario when conditions inspired to $SO(10)$ grand unification theories are considered, also in combination with the strong thermal condition. In both cases, interesting results on the low-energy neutrino parameters are obtained, representing predictions that can be tested in the future experiments.

We have shown that the theoretical request of full independence of initial condition is able to constrain the parameters space and give interesting results on neutrino masses and mixing. This goes in the direction of the need for "testable" leptogenesis models. It is evident that the restriction to a minimal scenario of leptogenesis, like that provided by type-I seesaw, is not enough to get solid predictions, even when asking for successful leptogenesis. This can be avoided when strong thermal leptogenesis is required. This condition focuses the attention on the so-called N_2-dominated scenario, with the heavy neutrino spectrum as in eq. (2.5). This scenario is often neglected when dealing with leptogenesis, because one may expect that the washout by the lightest neutrino totally erases the lepton asymmetry generated by the next-to-lightest. However, it can be shown that this is not true when flavour effects are considered, so that the asymmetry can survive N_1's washout in some flavour directions, along which the washout is mild. This must not be regarded as fine-tuned, since successful leptogenesis can be produced by a flavoured N_2-dominated scenario in around 30% of the parameter space [5, 6].

Moreover, in this scenario, favourable values of the absolute neutrino mass scale are found for NO, $m_1 \gtrsim 10\,\mathrm{meV}$ and IO, $m_1 \gtrsim 3$ meV. In NO a further analytical lower bound is found for natural choices of Ω ($M_\Omega \lesssim 4$), see eq. (3.14), while in IO the analytical threshold is obtained only for $M_\Omega \lesssim 0.9$. These constraints on m_1 allow the future cosmological observations, together with the determination of the neutrino mass ordering, to test strong thermal leptogenesis. The inclusion of corrective effects such as flavour coupling further constrains the statistical bound on m_1.

When $SO(10)$-inspired conditions are taken into account, a much richer landscape of predictions arises. These predictions, first obtained numerically, have all been confirmed and proved analytically. $SO(10)$-inspired leptogenesis implies interesting bounds on the absolute neutrino mass scale and on the atmospheric mixing angle θ_{23}. When strong thermal leptogenesis is con-

sidered on top of the $SO(10)$-inspired conditions, the bounds are even strengthened. In particular, inverted ordering is ruled out, fourth-quadrant values of the Dirac *CP*-violating phase, $\delta \simeq -\pi/4$, are favoured and first-octant atmospheric mixing angle, $\theta_{23} \lesssim 41^\circ$, are predicted.

All these predictions fall within the reach of future experiments or cosmological observations, therefore strong thermal $SO(10)$-inspired leptogenesis will be almost completely tested during the next years. The results from the NOνA experiment [26] and the T2K constraints on δ and θ_{13} [27] will allow to test the low-energy predictions of strong thermal $SO(10)$-inspired leptogenesis. At the same time, cosmological observations will be able to test the narrow window $75\,\text{meV} \lesssim \sum_i m_i \lesssim 125\,\text{meV}$ allowed by this solution. Moreover, in a more distant future, also $0\nu\beta\beta$ experiment will be able to study the range predicted by this solution and centred around $m_{ee} \simeq 15\,\text{meV}$. Only the Majorana phases ρ and σ will remain out of the testability reach.

This shows that the requirement of full independence of the initial conditions (strong thermal leptogenesis), together with the conditions inspired to $SO(10)$ grand unification theories, enable us to seriously put to test leptogenesis and the seesaw mechanism, thus casting more light on the origin of neutrino masses and mixing.

References

[1] M. Fukugita and T. Yanagida, Phys. Lett. B **174** (1986) 45.

[2] P. A. R. Ade *et al.* [Planck Collaboration], arXiv:1502.01589 [astro-ph.CO].

[3] P. Di Bari, Nucl. Phys. B **727** (2005) 318 [hep-ph/0502082].

[4] W. Buchmuller, P. Di Bari and M. Plumacher, Annals Phys. **315** (2005) 305 [hep-ph/0401240].

[5] M. Re Fiorentin and S. E. King, arXiv:1405.2318 [hep-ph].

[6] P. Di Bari S. E. King and M. Re Fiorentin, *in preparation*

[7] S. Blanchet, P. Di Bari, D. A. Jones and L. Marzola, JCAP **1301** (2013) 041 [arXiv:1112.4528 [hep-ph]].

[8] O. Vives, Phys. Rev. D **73** (2006) 073006 [hep-ph/0512160]; S. Blanchet and P. Di Bari, Nucl. Phys. B **807** (2009) 155 [arXiv:0807.0743 [hep-ph]];

[9] M. Yoshimura, Phys. Rev. Lett. **41** (1978) 281 [Erratum-ibid. **42** (1979) 746]. S. Dimopoulos and L. Susskind, Phys. Rev. D **18** (1978) 4500. D. Toussaint, S. B. Treiman, F. Wilczek and A. Zee, Phys. Rev. D **19** (1979) 1036. E. W. Kolb and S. Wolfram, Nucl. Phys. B **172** (1980) 224 [Erratum-ibid. B **195** (1982) 542]. E. W. Kolb, A. D. Linde and A. Riotto, Phys. Rev. Lett. **77** (1996) 4290 [hep-ph/9606260].

[10] R. Kallosh, A. D. Linde, D. A. Linde and L. Susskind, Phys. Rev. D **52** (1995) 912 [hep-th/9502069]. H. Davoudiasl, R. Kitano, G. D. Kribs, H. Murayama and P. J. Steinhardt, Phys. Rev. Lett. **93** (2004) 201301 [hep-ph/0403019].

[11] I. Affleck and M. Dine, Nucl. Phys. B **249** (1985) 361.

[12] S. Antusch, P. Di Bari, D. A. Jones and S. F. King, Nucl. Phys. B **856** (2012) 180 [arXiv:1003.5132 [hep-ph]].

[13] E. Bertuzzo, P. Di Bari and L. Marzola, Nucl. Phys. B **849** (2011) 521 [arXiv:1007.1641 [hep-ph]].

[14] P. Di Bari and L. Marzola, Nucl. Phys. B **877** (2013) 719 [arXiv:1308.1107 [hep-ph]].

[15] P. Di Bari, S. King and M. Re Fiorentin, JCAP **1403** (2014) 050 [arXiv:1401.6185 [hep-ph]].

[16] J. A. Casas and A. Ibarra, Nucl. Phys. B **618** (2001) 171 [hep-ph/0103065].

[17] J. Hamann, S. Hannestad and Y. Y. Y. Wong, JCAP **1211** (2012) 052 [arXiv:1209.1043 [astro-ph.CO]].

[18] P. Di Bari and M. Re Fiorentin, *in preparation*

[19] W. Buchmuller and M. Plumacher, Phys. Lett. B **389** (1996) 73 [hep-ph/9608308]; E. Nezri and J. Orloff, JHEP **0304** (2003) 020 [hep-ph/0004227]; G. C. Branco, R. Gonzalez Felipe, F. R. Joaquim and M. N. Rebelo, Nucl. Phys. B **640** (2002) 202 [hep-ph/0202030]; E. K. Akhmedov, M. Frigerio and A. Y. Smirnov, JHEP **0309** (2003) 021 [hep-ph/0305322].

[20] P. Di Bari and A. Riotto, JCAP **1104** (2011) 037 [arXiv:1012.2343 [hep-ph]].

[21] F. P. An *et al.* [DAYA-BAY Collaboration], Phys. Rev. Lett. **108** (2012) 171803 [arXiv:1203.1669 [hep-ex]].

[22] F. Capozzi, G. L. Fogli, E. Lisi, A. Marrone, D. Montanino and A. Palazzo, Phys. Rev. D **89**, no. 9, 093018 (2014) [arXiv:1312.2878 [hep-ph]].

[23] M. C. Gonzalez-Garcia, M. Maltoni and T. Schwetz, JHEP **1411**, 052 (2014) [arXiv:1409.5439 [hep-ph]].

[24] P. Di Bari, L. Marzola and M. Re Fiorentin, Nucl. Phys. B **893**, 122 (2015) [arXiv:1411.5478 [hep-ph]].

[25] P. Di Bari, L. Marzola, Talks at the DESY Theory Workshop, 2011, http://th-workshop2011.desy.de/.

[26] R. B. Patterson [NOvA Collaboration], Nucl. Phys. Proc. Suppl. **235-236** (2013) 151 [arXiv:1209.0716 [hep-ex]].

[27] K. Abe *et al.* [T2K Collaboration], Phys. Rev. Lett. **112** (2014) 061802 [arXiv:1311.4750 [hep-ex]].